ORGANIC LETTERS

2012
Vol. 14, No. 24
6282–6285

Polymorphic Equilibrium Responsive Thermal and Mechanical Stimuli in Light-emitting Crystals of *N*-Methylaminonaphthyridine

Naomi Harada, Yuichiro Abe, Satoru Karasawa, and Noboru Koga*

Graduate School of Pharmaceutical Sciences, Kyushu University, 3-1-1 Maidashi, Higashi-ku, Fukuoka, 812-8582 Japan.

koga@fc.phar.kyushu-u.ac.jp

Received November 6, 2012

ABSTRACT

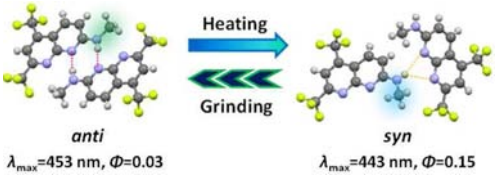

Crystal polymorphs of 1,8-naphthyridine derivative, being *anti* and *syn* conformers, show a reversible transformation from *anti* to *syn* by heating and from *syn* to *anti* by grinding with the alteration of emittance intensity, and notably, thermal transformation from *anti* to *syn* conformer took place in single-crystal-to-single-crystal (SC-to-SC) form, which was confirmed by a single crystal X-ray crystallography.

The solid-state emissions of organic molecules and metal complexes in response to heat,[1] pressure,[2] light,[3] etc.[4] have drawn attention and intensive study. Since the solid-state emitting properties strongly depend on the molecular structure and the molecular arrangements in crystals, the alteration of molecular arrangements caused by external stimuli (heat, pressure, light, etc.) manifests as changes observed in emission color and intensity. In crystal polymorphs, transformation between them by external stimuli produces alterations of emitting color and intensity. Therefore, many molecules and metal complexes showing polymorph-dependent emission have been reported as switchable molecules by taking advantage of crystal-to-crystal (C-to-C) interconversion.[5]

However, the examples that single-crystal-to-single-crystal (SC-to-SC) phase transition have been limited.[6] Recently, we reported the donor−acceptor type of quinoline (TFMAQ) derivatives showing an emission color change with exothermic SC-to-SC transformation.[6b] In the polymorphs of 1,8-naphthyridine derivative, this time, endothermic SC-to-SC transformation with alteration of the emission intensity was observed. We report herein the solid-state (crystalline) emitting properties of polymorphs of 1,8-naphthyridine fluorophores in response to heat and grinding.

Formula

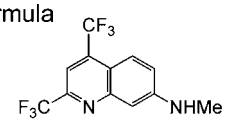

TFMAQ-NHMe

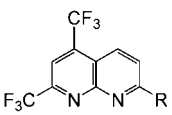

1; R = NH_2 **2**; R = NHMe

A parent compound, 2,4-ditrifluoromethyl-7-amino-1,8-naphthyridine, **1**, was prepared in a manner similar to the

(1) (a) Zhao, Y.; Gao, H.; Fan, Y.; Zhou, T.; Su, Z.; Liu, Y.; Wang, Y. *Adv. Mater.* **2009**, *21*, 3165–3169. (b) Chung, J. W.; An, B.-K.; Park, S. Y. *Chem. Mater.* **2008**, *20*, 6750–6755. (c) Mutai, T.; Satou, H.; Araki, K. *Nat. Mater.* **2005**, *4*, 685–687.

(2) (a) Zhang, G.; Lu, J.; Sabat, M.; Fraser, C. L. *J. Am. Chem. Soc.* **2010**, *132*, 2160–2162. (b) Ito, H.; Saito, T.; Oshima, N.; Kitamura, N.; Ishizuka, S.; Hinatsu, Y.; Wakeshima, M.; Kato, M.; Tsuge, K.; Sawamura, M. *J. Am. Chem. Soc.* **2008**, *130*, 10044–10045. (c) Sagara, Y.; Mutai, T.; Yoshikawa, I.; Araki, K. *J. Am. Chem. Soc.* **2007**, *129*, 1520–1521.

(3) (a) Chung, J. W.; You, Y.; Huh, H. S.; An, B.-K.; Yoon, S.−J.; Kim, S. H.; Lee, S. W.; Park, S. Y. *J. Am. Chem. Soc.* **2009**, *131*, 8163–8172. (b) Kumar, N. S. S.; Varghese, S.; Narayan, G.; Das, S. *Angew. Chem., Int. Ed.* **2006**, *45*, 6317–6321.

(4) Crenshaw, B. R.; Weder, C. *Chem. Mater.* **2003**, *15*, 4717–4724.

(5) (a) Mutai, T.; Tomoda, H.; Ohkawa, T.; Yabe, Y.; Araki, K. *Angew. Chem., Int. Ed.* **2008**, *47*, 9522–9524. (b) Davis, R.; Rath, N. P.; Das, R. *Chem. Commun.* **2004**, 74–75.

(6) (a) Luo, X.; Li, J.; Li, C.; Heng, L.; Dong, Y. Q.; Liu, Z.; Bo, Z.; Tang, B. Z. *Adv. Mater.* **2011**, *23*, 3261–3265. (b) Abe, Y.; Karasawa, S.; Koga, N. *Chem.—Eur. J.* **2012**, *18*, 15038–15048.

10.1021/ol302963e
Published on Web 12/12/2012

procedure for TFMAQ using 2,6-diaminopyridine in place of 1,3-diaminobenzene.[6b] Amino moiety of **1** was converted to chloride, via hydroxy derivative,[7] followed by reaction with methylamine in the presence of copper catalyst to afford **2** in 59% yield (4 steps, Scheme S1, Supporting Information). From recrystallization with a mixture of *n*-hexane and CH_2Cl_2 for **2**, single crystals were obtained as yellowish plates. In solution, fluorophores **1** and **2** showed emission depending on the solvent polarity. Fluorescence emission at λ^f_{max} (Φ_f) = 392 (0.04), 406 (0.14), 416 (0.19), and 435 (0.40) nm for **1** and at λ^f_{max} (Φ_f) = 389 (0.09), 432 (0.36), 436 (0.50), and 444 (0.33) nm for **2** in *n*-hexane, chloroform, ethyl acetate, and methanol, respectively, were observed under irradiation at 380 nm (Figure S1, Supporting Information). In solid states, on the other hand, **1** and **2** showed weak blueish emission. Interestingly, the emission intensity of the crystalline sample of **2** increased by heating at 200 °C. Photographs of a single crystal taken under a microscope are shown in Figure 1.

Since the observed thermal emitting behavior suggested a SC-to-SC transformation between the polymorphs, X-ray crystallography was carried out. By heating a large sized crystal (5 × 3 × 3 mm) of pale yellow plate, **2b**, at 200 °C, the crystal was partially destroyed. The obtained crystal was cut and used as sample of **2a** for X-ray crystallography. The single crystal of **2a** was also obtained by sublimation of crystal **2b** at over 150 °C. X-ray crystallography (monoclinic, $P2_1/c$, and $Z = 4$) indicated that **2b** and **2a** were polymorphous and that the *a*, *b*, and *c* axes for crystal **2b** corresponded to the *b*, *a*, and *c* axes for crystal **2a** (Figure S2, Supporting Information). The molecular and crystal structures for **2b** and **2a** revealed by X-ray crystallography are shown in Figure 2. In the molecular structure, the molecule of **2b** was an *antiperiplanar* (*anti*) conformer in relation to the methyl moiety, while that of **2a** was a *synperiplanar* (*syn*) conformer. Interestingly, the observed thermal transformation from **2b** (*anti*) to **2a** (*syn*) was opposite to that for the corresponding TFMAQ-NHMe, in which thermal SC-to-SC transformation took place from the *syn* to *anti* conformer. In the molecular packings for **2b** and **2a**, the short distances (r_{N-N1} and r_{N-N8}) between the nitrogen of amine and that at the 1- and

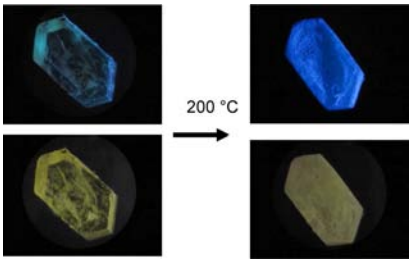

Figure 1. Photographs of a single crystal of **2** before (left) and after (right) heating at 200 °C for 10 min. Upper and lower show under the irradiation at 365 nm and the room light, respectively.

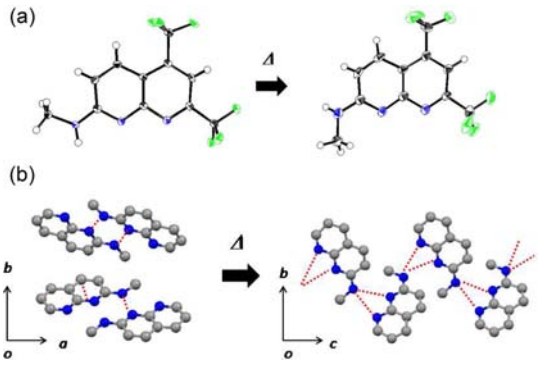

Figure 2. (a) ORTEP drawings of molecular structures of **2b** (left) and **2a** (right) and (b) molecular packings for **2b** (left) and **2a** (right) in a ball and stick model, In (b), H atoms and CF_3 groups are omitted. Dotted lines indicate hydrogen bonds.

8-positions of naphthyridine belonging to the other molecule were observed and expected to form the hydrogen bonds. In **2b**, the molecules formed the head-to-tail dimer through the hydrogen bonds in the distance (r_{N-N8}) of 2.99 Å. In contrast, the molecules of **2a** formed one-dimensional hydrogen bonding in the distances of r_{N-N1} = 3.14 and r_{N-N8} = 3.15 Å along the *c* axis. The molecular arrangements for **2b** and **2a** showed different types of herringbone (HB) structures along the *c* and *a* axes, respectively. **2b** was classified as γ-HB structure from the length of the shortest axis (Figure S3, Supporting Information).[8] The differences of the packing arrangements with different hydrogen bonding in **2b** and **2a** might affect the emitting properties.

The fluorescence spectra of the crystal (crushed) sample of **2b** showed the weak emission at λ^f_{max} of 459 nm with Φ_f(cry) of 0.03, while **2a** showed a blue shift by 10 nm and a increase in Φ_f(cry), and values of λ^f_{max} of 444 nm and Φ_f(cry) of 0.15, were obtained . The spectral changes are shown in Figure 3a together with the absorption spectra. The blue shift of the emission with the increase of the fluorescence intensity for **2a** might be due to the alteration from a strong hydrogen bonded dimer to weak hydrogen bond chains. Subsequently, when the obtained **2a** (ca. 1 mg) was ground with an agate mortar and a pestle for 10 min, the emission intensity decreased and the wavelength returned to 463 nm (Figure S4, Supporting Information), suggesting that **2a** returned to **2b** by a mechanical stimulus. The formation of **2b** was also supported by IR spectra, in which the absorption at 3301 cm^{-1} due to the NH stretching for **2a** shifted to ~3200 cm^{-1} for **2b** by grinding (Figure 3b). It is noted that the observed shift to the low wavenumber indicated the phase transition to a species having strong hydrogen bond. By repeating the cycle of

(7) Newkome, G. R.; Garbis, S. J.; Majestic, V. K.; Fronczek, F. R.; Chiari, G. *J. Org. Chem.* **1981**, *46*, 833–839.

(8) (a) Hunter, C. A.; Lawson, K. R.; Perkins, J.; Urch, C. J. *J. Chem. Soc., Perkin Trans. 2* **2001**, 651–669. (b) Gavezzotti, A.; Desiraju, G. R. *Acta Crystallogr., Sect. B* **1989**, *45*, 473–482.

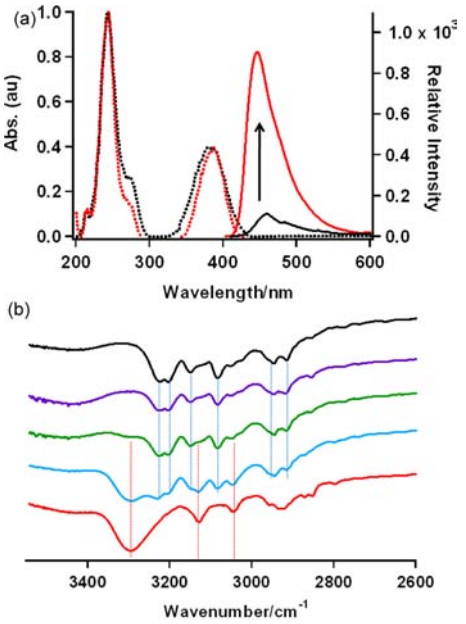

Figure 3. (a) Emission (solid line) and absorption (dotted line) spectra before (black) and after (red) heating **2b** and (b) change of IR spectra of **2a** before (red), after grinding for 5 min (sky blue), 10 min (green), 15 min (purple), and **2b** (blue). Solid-line bars indicate the absorption due to **2a** (red) and **2b** (blue).

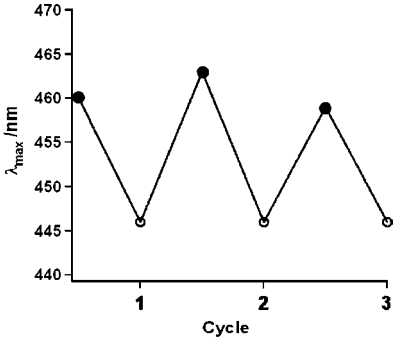

Figure 4. Change of λ^{f}_{max} value after heating at 200 °C (○) and grinding (●) in the heat-grinding cycles.

heating–grinding, the alteration of emission could be representative (Figure 4).

To investigate the thermal properties and the structural alterations after heating and grinding, differential scan calorimetry (DSC) and X-ray diffraction (XRD) measurements of **2b** and **2a** were carried out. DSC were measured in the temperature range 25–250 °C for three cycles of heating and cooling (10 °C/min for heating and cooling rate, Figure 5). In the first cycle for **2b**, DSC curves showed weak and strong endothermic peaks at 177 and 228 °C, respectively, on heating and a strong exothermic peak at 217 °C on cooling. The peaks at 228 and 217 °C were due to the melting and the solidification, respectively. Interestingly, a weak peak at 177 °C indicating as endothermic phase transition suggested that an enantiotropic transition between two polymorphs took place.[9] In the second and the third cycles, no additional peak at 177 °C was observed, suggesting that **2a** formed after melting. In contrast, the corresponding peak for TFMAQ-NHMe was exothermic, suggesting a monotropic transition.[10] To determine the exothermic peak due to the transition from **2a** to **2b**, the cooling processes after heating at 200 °C and after melting at 228 °C were carefully investigated until 0 °C (2 °C/min). In both measurements, no exothermic peak was observed. The lack of a peak due to the transition from **2a** to **2b** indicated that the crystal polymorph **2a** formed after heating at 200 °C and melting was thermally stable and did not spontaneously return to **2b** above 0 °C. Polymorph **2a** also showed DSC curves similar those in the second and third cycles for **2b** (Figure S6, Supporting Information).

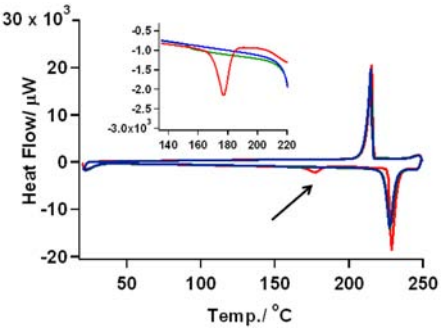

Figure 5. DSC curves of **2b**. (Inset) the range of 135–220 °C indicated by the arrow is expanded.

The XRD measurements using one sample of **2b** were continually carried out in order of (i) the sample of powder, (ii) after heating the powder at 200 °C for 10 min, (iii) after melting and cooling to rt and (iv) after grinding for 60 min. The changes of XRD patterns of **2b** are shown in Figure 6. Before heating, the XRD pattern of the powder sample (Figure 6i) was consistent with that simulated from the result of single crystal X-ray analysis. After heating at 200 °C, the XRD pattern was changed and new peaks were observed (Figure 6ii) which were consistent with that for **2a**. After melting and cooling to rt, the XRD pattern was also consistent with that for **2a** (Figure 6iii), indicating that **2a** formed after melting. This result might be because the solidifying temperature (217 °C) was higher than the phase-transfer one (177 °C). Interestingly, the XRD pattern after grinding the sample at (iii) was close to that for **2b** (Figure 6iv), indicating that **2a** returned to **2b** by grinding.

The results of DSC and XRD suggested that the transformation from **2b** to **2a** above 200 °C took place. Furthermore, XRD in addition to the alteration of emission and IR absorption indicated that **2a** obtained by heating returned to **2b** in response to mechanical stimulus

(9) Mehta, G.; Sen, S. *Chem. Commun.* **2009**, 5981–5983.
(10) Céolin, R.; Tamarit, J.-L.; Barrio, M.; López, D. O.; Nicolaï, B.; Veglio, N.; Perrin, M.-A.; Espeau, P. *J. Pharm. Sci.* **2008**, *97*, 3927–3941.

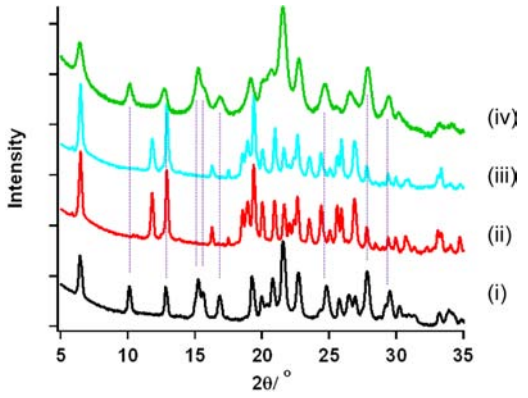

Figure 6. XRD pattern changes for powder sample of **2b**; (i) the sample of powder, (ii) after heating at 200 °C for 10 min and cooling to rt, (iii) after melting and cooling to rt, and (iv) after grinding for 60 min.

of grinding. Therefore the polymorphs **2b** and **2a** showed the reversibility in that **2b** converted to **2a** by heating, while the resulting **2a** returned to **2b** by grinding. The observed reversibility might be due to the thermal phase transition, in which **2b** and **2a** were enthalpically and entropically stable, respectively. At room temperature, **2a** was entropically unstable, and a subtle stimulus such as grinding might be a sufficient trigger to induce transformation to the enthalpically stable **2b**.

In conclusion, crystal polymorphs, **2b** and **2a**, emitting different intensities, reversibly transformed from **2b** to **2a** by heating and from **2a** to **2b** by grinding. Especially, thermal conversion from **2b** to **2a** took place in SC-to-SC. The emitting intensity for **2a** was 5 times larger than that for **2b**, and the accompanying thermal and mechanical phase transitions could be regard as a switchable emission.

Supporting Information Available. Experimental details, absorption and emission spectra of **1** and **2** in various solvents and solid state, the molecular packings for **2**, photographs for the powders of **2b** and **2a**, and other data mentioned in this paper. This material is available free of charge via the Internet at http://pubs.acs.org.

The authors declare no competing financial interest.